Knockdown of hsa_circ_0074298 suppressed the progression of pancreatic cancer by targeting the miR-519/SMOC2 axis

Hong Chen (dr_chenhong@163.com)
Southeast University Zhongda Hospital https://orcid.org/0000-0002-0423-9807
Dafang Xu
Southeast University Zhongda Hospital
Lishan Wang
Southeast University Zhongda Hospital
Jiahua Zhou
Southeast University Zhongda Hospital

Primary research

Keywords: pancreatic cancer (PC), hsa_circ_0074298, miR-519, SMOC2, chemoresistance

Posted Date: May 7th, 2020

DOI: https://doi.org/10.21203/rs.2.23308/v4

Abstract

BACKGROUND: Pancreatic cancer (PC) is among the most malignant tumors in the digestive system because of its fast progression, metastasis, as well as its resistance to chemotherapy. Former studies found that circRNAs that were differentially expressed were correlated with progression and gemcitabine (GEM)-resistance in PC, and hsa_circ_0074298 aberrant expression played a role in PC progression, but the regulatory mechanism was unclear.

METHODS: RT-qPCR was used to detect hsa_circ_0074298 expression in PC cell lines. CCK8, colony formation, and Transwell assays were used to evaluate the effect of hsa_circ_0074298 on PC cell migration and proliferation. Bioinformatics and luciferase reporter experiments were used to characterize the regulatory mechanism. Nude mouse xenografts were generated to examine the effect of hsa_circ_0074298 on tumor growth.

RESULTS: The present study showed that hsa_circ_0074298 expression increased significantly in both PC cell lines and PC tissues. Downregulation of hsa_circ_0074298 caused a significant decrease in PC cell proliferation and in nude mouse xenograft growth. Hsa_circ_0074298 silencing also increased chemotherapy sensitivity to GEM. Bioinformatics analysis indicated that hsa_circ_0074298 was a miR-519 sponge and that the *SMOC2* gene was a miR-519 target. MiR-519 downregulation or SMOC2 overexpression restored cell proliferation, migration, and chemoresistance after hsa_circ_0074298 silencing. The dual luciferase reporter assay showed that hsa_circ_0074298 interacted with miR-519, and miR-519 binding to the SMOC2 3'-UTR then suppressed posttranscriptional SMOC2 expression.

CONCLUSIONS: Taken together, hsa_circ_0074298 functioned as a tumor promoter through a novel miR-519/SMOC2 axis, highlighting its possibility as a potential therapy for PC.

Background

Pancreatic cancer (PC) is among the major causes of cancer-relevant mortality in the world. Mortality caused by PCs of various classes accounted for 411,600 deaths in 2015 [1]. Multiple rounds of chemotherapy using gemcitabine (GEM) is now a common adjunct treatment for PC. However, resistance to GEM is a major obstacle for effective chemotherapy of PC [2-4], although the molecular mechanism of PC resistance to GEM is still unclear.

Non-coding RNAs (ncRNAs) are RNAs which do not encode proteins. It is already known that ncRNA contributes to a large amount of cellular RNAs, making at least 90% of human RNAs [5]. Former studies have shown that ncRNAs, like proteins, act as underlying factors in various cellular processes, including cell migration, proliferation, apoptosis, chemoresistance, angiogenesis, and the immune response [6, 7]. CircRNAs are considered as essential human disease regulators as well as biomarkers in many kinds of malignancies such like PC. The competing endogenous RNA (ceRNA) mechanism is known as an indispensable mechanism through which circRNAs regulate gene expression. Theoretically, circRNAs are molecular sponges for miRNA with its binding site indirectly regulating gene expression [8-11].

Previous studies have found that circular RNA circ_0007534, which regulates cell apoptosis, invasion, as well as proliferation by sponging miR-892b and miR-625 [12], is upregulated and associated with an unfavorable prognosis in pancreatic ductal adenocarcinoma patients. CircRNA_100782 regulates pancreatic carcinoma proliferation via the IL6-STAT3 pathway [13]. Previous studies with microarray analysis involving circRNA expression profiles associated with GEM resistance in PC cells also revealed a family of circRNAs that were differentially expressed, including hsa_circ_0074298 [14]. Although hsa_circ_0074298 functions in PC progression, its mechanism of GEM resistance is not clear. In the current investigation, our aim was to identified the regulatory mechanism of hsa_circ_0074298.

Materials & Methods

Ethics statement

We collected 30 fresh PC tissues and paired adjacent tissues after obtaining informed consent from patients at the Affiliated Zhongda Hospital, Southeast University, Nanjing. We snap-froze samples in liquid nitrogen and stored them at -80°C before RNA extraction and fluorescence *in situ* hybridization (FISH). The Ethics Committee of the Affiliated Zhongda Hospital of Southeast University (Nanjing, China) approved this research, and the study was carried out in accordance with The Code of Ethics of the World Medical Association. The ethic approval code was 2016ZDSYLL027.0.

Fluorescence in situ hybridization (FISH)

We prepared particular probes to hsa_circ_0074298 (Dig-5'-GCCTCAACCACGGAGTTCCTTTTGCTCGG-3'-Dig) by Geneseed Biotech (Guangzhou, China). We detected signals using fluorescein isothiocyanate (FITC)-conjugated anti-biotin antibodies and Cy3-conjugated anti-digoxin antibody (Jackson ImmunoResearch, West Grove, PA, USA). We counterstained nuclei with 4,6-diamidino-2-phenylindole, and obtained images using a Zeiss LSM 700 confocal microscope (Carl Zeiss, Oberkochen, Germany).

Cellculture

We obtained PC cell lines (PANC-1, SW1990, AsPC-1, and BxPC-3) as well as normal human pancreatic duct epithelial (HPDE) cells from the American Type Culture Collection. The culture medium consisted of 10% fetal bovine serum (FBS; Invitrogen Life Technologies, Carlsbad, CA, USA) and penicillin in Dulbecco's modified Eagle's medium. We cultured the cells in an incubator at 37°C with 5% CO_2.

Bioinformatics analyses

We predicted circRNA/miRNA target genes using *Circular RNA Interactome*, and predicted the interactive relationships between miR-519 and SMOC2 using *TargetScanHuman*.

Celltransfection

The cDNA oligonucleotides specifically targeting hsa_circ_0074298 (sh-circ0074298), miR-519 inhibitor, and SMOC2 overexpression vector were synthesized by GenePharma (Shanghai, China). Both sh-circ0074298 and SMOC2 overexpression vectors were inserted into pcDNA3.1. Expression of hsa_circ_0074298, miR-519, and SMOC2 were then monitored using RT-qPCR and western blotting after transfection of PC cells for 48 h.

Lentivirus transfection assay

The full-length cDNA cloning vector was purchased from GenePharma (Shanghai, China) and used for the amplification template. The SMOC2 full-length cDNA was amplified with NheI and BamH I restriction sites using KOD-PLUS Neo polymerase. Then, the PCR-amplified cDNA was cloned into the pcDNA3.1 vector using restriction enzymes and DNA ligase. The sh-circ0074298 sequence were also inserted into the pcDNA3.1 vector. The recombined vector was packed with VSV, REV, and GAG vectors and transfected into 293T cells using the Lipofectamine 2000 Reagent (Invitrogen) to obtain a virus supernatant. The virus supernatant was added into PANC-1 cells with polybrene. The transfected PANC-1 cells were cultured with puromycin and verified by western blotting or an RT-qPCR assay [15].

Transwell migration and invasion assay

We analyzed cell migration using Transwell chambers (8 μm, 24-well plates) (Corning, Corning, NY, USA) following standard procedures. Cells (1×10^4 cells) were added to the upper chamber and cultured for 24 h, then removed from the chamber upper surfaces using cotton swabs. We fixed the cells located on the lower surfaces with methanol for 10 min, followed by Crystal Violet staining. We imaged the stained cells and counted them in five fields, which were randomly selected. For the invasion experiments, we coated the chamber inserts with 200 mg/mL diluted Matrigel and dried them overnight under sterile conditions.

RNAextractionandRT-qPCR

We utilized TRIzol reagent (Invitrogen Life Technologies) to separate total RNA from cultured PC cells and tissues as previous research described [16]. The RNA concentrations were measured with a NanoDrop 2000 Spectrophotometer (Nano Drop Technologies, Wilmington, DE, U.S.A.) and 500 ng total RNA or miRNA was reverse transcribed into cDNA using the High Capacity RNA to cDNA Kit (Takara Biotechnology Co., Ltd., Dalian, China) or the microRNA Reverse Transcription kit (Takara Biotechnology Co., Ltd.). The primers used for RT-qPCR were: hsa_circ_0074298, forward: 5'-TTATTGATTATTACTGGCAAAAACG-3', reverse: 5'-CTATGTGGTAGCGTTTAATGTTGGT-3'; miR-519, RT primer, 5'-GTCGTATCCAGTGCGTGTCGTGGAGTCGGCAATTGCACTGGATACGACCACTCT-3'; miR-519d, forward: 5'-CAAAGTGCCTCCCTTT-3' and reverse: 5'-CAGTGCGTGTCGTGGAGT-3'; glyceraldehyde 3-phosphate dehydrogenase (GAPDH), forward: 5'-CCAAAATCAGATGGGGCAATGCTGG-3' and reverse: 5'-TGATGGCATGGACTGTGGTCATTCA-3'; and U6, forward: 5'-CTCGCTTCGGCAGCACATA-3' and reverse: 5'-AACGATTCACGAATTTGCTG-3'. The thermal cycle was: 30 s at 95˚C, 5 s for 40 cycles at 95˚C, and 35 s at 60˚C.

Cellproliferationassay

Following the CCK-8 assay (Dojindo Laboratories, Kumamoto, Japan), we assessed cell growth of transfected cells in plates with 96 wells at 24, 48, and 72 h. We used a spectrophotometer (Thermo Scientific, Rockford, IL, USA) to detect the absorbance at 450 nm.

Colonyformationassay

We transferred BxPC-3 and PANC-1 cells into plates with 6 wells for 10 days. Then, we treated the colonies with 10% formaldehyde for 30 min, followed by staining for 5 min with 0.5% Crystal Violet. Image-Pro Plus 6.0 (https://www.mediacy.com/imageproplus) was used for data analysis.

Cellcycleassay

A total of 2×10^5 cells/mL were diluted with RNase A in 75% ice-cold ethanol overnight, then stained with propidium iodide (PI; 50 mg/mL; MultiSciences Biotech, Hangzhou, China) in the dark for 30 min at 4ºC, followed by measuring with a flow cytometer (FACScan, BD Bioscience, San Jose, CA, USA).

Cellapoptosisassay

Flow cytometry binding buffer (100 µL) was added after harvested cells were washed twice using ice-cold buffer. The mixture containing 5 µL Annexin V/FICC and PI (BD, Franklin Lakes, NJ, USA) was used for staining of cells for 15 min in the dark, followed by 400 µL of binding buffer. We used a FACSCalibur flow cytometer (BD Biosciences) to analyze cell apoptosis.

Westernblotanalysis

We washed cells with precooled phosphate-buffered saline and then lysed them with cell lysis solution (RIPA). We detected the protein concentration via BCA (Thermo Fisher Scientific, Waltham, MA, USA). We then transferred proteins to a polyvinylidene difluoride membrane, and blocked them in TBST (25 mM Tris, 140 mM NaCl, and 0.1% Tween 20, pH 7.5) containing 5% skimmed milk and then incubated them for 2 h. We then incubated membranes in primary antibodies against SMOC2 and GAPDH (Abcam, Cambridge, MA, U.S.A.) at 4°C overnight. After washing (3× for 10 min) with TBST, we added secondary antibody and incubated them at room temperature for 1 h. The results were analyzed using ImageJ software (National Institutes of Health, Bethesda, MD, USA).

Dual-luciferase reporter assay

We cloned the putative miR-519 binding site in the target gene, *SMOC2*, and wild-type (WT) or mutant (MUT) hsa_circ_0074298 3'-UTR into the psi-CHECK (Promega, Madison, WI, USA) vector downstream of the firefly luciferase 3'-UTR, or hsa_circ_0074298 as a primary luciferase signal with Renilla luciferase for the normalization signal, and named them as SMOC2-Wt/circ-0074298-Wt and SMOC2-Mut//circ-0074298-Mut. The psi-CHECK vector provided the Renilla luciferase signal for normalization to

compensate for distinctions between harvested efficiencies and transfection. We performed transfection of HEK293 cells using Lipofectamine 2000 (Invitrogen Life Technologies, Carlsbad, CA, USA). We measured Renilla and firefly luciferase activities 1 day after transfection with the Dual-Luciferase Reporter Assay System (Promega, Mannheim, Germany) using a luminometer (Molecular Devices, San Jose, CA, USA), and analyzed relative Renilla luciferase activities following standard procedures.

Animal studies

For xenograft assays, we injected 1×10^6 modified (sh-circRNA, sh-circRNA + miR-519 inhibitor, or sh-circRNA + SMOC2) or control PANC-1 cells subcutaneously into male nude mice (Chinese Science Academy) in the right side. We measured tumor volumes (length × width^2 × 0.5) at the indicated time points, and excised tumors 4 weeks after injection. Each group was comprised of six mice.

We maintained all mice and handled them according to the instructions of the Animal Ethics Committee of Affiliated Zhongda Hospital of Southeast University (Nanjing, China).

Statisticalanalysis

We conducted statistical analysis using SPSS version 13.0 software (IBM, New York, NY, USA). We utilized Student's *t*-test to analyze the data, which are expressed as the mean ± SD. A value of $p < 0.05$ was regarded as statistically significant.

Results

The hsa_circ_0074298 knockdown suppressed PC proliferation using *in vitro* and *in vivo* experiments.

Bioinformatics analyses suggested that hsa_circ_0074298 was derived and cyclized from a portion of the *HARS* gene exon and was located at chr5:140053489-140058712 (Figure 1A). FISH detection showed that hsa_circ_0074298 expression increased in PC tissues when compared with their paired non-tumor tissues. Subcellular localization analysis showed that hsa_circ_0074298 was located predominantly in the cytoplasm (Figure 1B). We then performed qRT-PCR to determine hsa_circ_0074298 expression in 30 paired tissue specimens and four PC cells such as SW1990, BxPC-3, AsPC-1, and PANC1. We used HPDE cells as a control. The results showed that hsa_circ_0074298 expression increased in PC tissues (Figure 1C) and cell lines (Figure 1D). BxPC-3 and PANC-1 cells had the highest hsa_circ_0074298 expressions, which were used in subsequent assays. We conducted lentivirus-mediated hsa_circ_0074298 silencing of BxPC-3 and PANC-1 cells, and the results verified that hsa_circ_0074298 expression was significantly decreased (Figure 1E). Cell cycle distribution analysis showed that the percentage of S-phase cells significantly decreased and the percentage of G2/M-phase cells increased after hsa_circ_0074298 depletion, indicating a cell cycle arrest at the G2/M phase (Figure 1F). Both the CCK8 assay (Figure 1G and 1H) and colony formation assay (Figure 1I and 1J) showed that hsa_circ_0074298 depletion decreased cell proliferation in BxPC-3 and PANC-1 cells. PANC-1 cells transfected with or without hsa_circ_0074298 lentiviral interference vectors were used to assay tumor formation in nude mice

xenografts. We determined the results by measuring tumor volumes 5 days after grafting, with a Vernier caliper, and indicated that hsa_circ_0074298 knockdown resulted in a reduced xenograft volume (Figure 1K).

The hsa_circ_0074298 knockdown decreased migration capabilities and GEM resistances in PC.

The results confirmed that hsa_circ_0074298 depletion decreased the migration (Figure 2A and 2B) and invasion (Figure 2C and 2D) ability in BxPC-3 and PANC-1 cells. To define the degree of the PANC-1-derived GEM-resistant subclone PANC-1-GEM resistance, we treated the derived and parental cells with different GEM concentrations (0, 10, 25, 50, 100, and 200 nM). Cell viability was determined 2 days later using the CCK8 assay. The results showed that GEM inhibited the parental PANC-1 cell viability, but PANC-1-GEM cells were totally resistant, when using the highest GEM concentration of 200 nM (Figure 2E). CCK8 detection also showed that hsa_circ_0074298 depletion decreased the proliferative ability of PANC-1-GEM cells after 100 nM GEM treatment for different times (Figure. 2F). Flow cytometry analysis with FITC-conjugated Annexin V/PI staining showed that hsa_circ_0074298 depletion promoted cell apoptosis after treatment with 100 nM GEM for 48 h (Figure 2G and 2H). Overall, the results confirmed that hsa_circ_0074298 silencing inhibited PC cell migration and chemotherapy resistance, but the mechanism remains to be determined.

MiR-519/SMOC2 was the target of hsa_circ_0074298.

The bioinformatics analysis tool, *Circular RNA Interactome,* was used to select candidate hsa_circ_0074298 targets. The results confirmed that hsa_circ_0074298 had 12 more conservative miRNAs (miR-769-3p, miR-615-5p, miR-582-3p, miR-578, miR-572, miR-548p, miR-532-3p, miR-519, miR-515-3p, miR-510, miR-503, and miR-492) (Figure 3A). We then designed a hsa_circ_0074298 luciferase reporter screening protocol for the miRNAs. The results showed that miR-519 decreased the hsa_circ_0074298 luciferase reporter luciferase activity most by at least 80% (Figure. 3B). These results indicated that miR-519 had a more conserved binding site for hsa_circ_0074298. The RT-qPCR detection showed that miR-519 expression decreased in PC tissues when compared with adjacent non-tumor tissues (Figure 3C). We subsequently conducted a dual-luciferase reporter assay in HEK293T cells. We cloned mutant and wild-type hsa_circ_0074298 sequences to construct the mutant vectors and reporter plasmids, respectively (Figure. 3D). Although it was found that miR-519 mimics co-transfected with the reporter plasmids decreased luciferase activity, in contrast, miR-519 mimics and mutated vector transfection showed no significant changes in luciferase activity. Hence, these data proved that miR-519 was a direct hsa_circ_0074298 target (Figure 3E). Next, bioinformatics analysis (http://www.targetscan.org/) showed that SMOC2 was a potential miR-519 target. To confirm that SMOC2 was a miR-519 target, we cloned mutant and wild-type SMOC2 sequences to construct mutant vectors and reporter plasmids, respectively (Figure. 3F). The results showed that the reporter plasmid and miR-519 mimic co-transfections visibly suppressed luciferase activity and mutated SMOC2 vectors, but miR-519 mimic co-transfection had no significant effect on luciferase activity. These results proved that

miR-519 directly targeted SMOC2 (Figure. 3G), suggesting that miR-519/SMOC2 was the hsa_circ_0074298 target.

The miR-519 overexpression or SMOC2 downregulation reversed the hsa_circ_0074298 silencing suppressive effect on PC cell migration and proliferation.

RT-qPCR analysis validated that hsa_circ_0074298 expression was decreased after hsa_circ_0074298 silencing, but treatment with the overexpressing SMOC2 or the miR-519 inhibitor did not affect hsa_circ_0074298 expression (Figure. 4A and 4B), showing that miR-519 and SMOC2 were downstream of hsa_circ_0074298. RT-qPCR detection also verified that hsa_circ_0074298 silencing promoted miR-519 expression, but SMOC2 overexpression had no effect on hsa_circ_0074298 depletion-induced SMOC2 expression (Figure 4C and 4D), showing that SMOC2 was downstream of miR-519. Western blot analysis showed that hsa_circ_0074298 silencing decreased SMOC2 expression, but miR-519 inhibitor treatment reversed the inhibiting effect of hsa_circ_0074298 depletion on SMOC2 expression. After transfection with the SMOC2 overexpression vector, SMOC2 expression increased significantly (Figure 4E and 4F), suggesting that hsa_circ_0074298 promoted SMOC2 expression via sponging miR-519.

CCK8 assays (Figure 4G and 4H) and colony formation assays (Figure 4I-K) showed that downregulation of miR-519 restored the proliferative ability in PANC-1 and BxPC-3 cells after hsa_circ_0074298 depletion. SMOC2 overexpression significantly promoted cell proliferation in BxPC-3 and PANC-1 cells even after downregulation of hsa_circ_0074298 expression. The Transwell assay for migration analysis showed that downregulation of miR-519 restored the migration ability in PANC-1 and BxPC-3 cells after hsa_circ_0074298 depletion.

The *in vivo* xenograft mouse models using PANC-1 cells also showed that downregulation of miR-519 or upregulation of SMOC2 recovered the tumor growth ability of PANC-1 after hsa_circ_0074298 knockdown (Figure. 5A-C), suggesting that miR-519/SMOC2 was a hsa_circ_0074298 downstream target.

Furthermore, inhibition of miR-519 expression partially recovered cell migration and invasion after downregulation of hsa_circ_0074298. SMOC2 overexpression significantly promoted cell migration and invasion in PANC-1 and BxPC-3 cells, even after downregulation of hsa_circ_0074298 expression (Figure 5D-H). Overall, the results showed that Hsa_circ_0074298 promoted PC progression through sponging miR-519 and enhancing SMOC2 expression.

The miR-519 overexpression or SMOC2 downregulation reversed the hsa_circ_0074298 depletion suppressive effect on PC chemotherapy resistance.

The *in vivo* xenograft mouse models using PANC-1 cells also showed that downregulation of miR-519 or upregulation SMOC2 recovered the tumor growth ability of PANC-1 after hsa_circ_0074298 knockdown (Figure 4O), suggesting that miR-519/SMOC2 was a downstream target of the hsa_circ_0074298. The results verified that Hsa_circ_0074298 promoted PC progression by sponging miR-519 and enhancing SMOC2 expression.

CCK8 assay results also showed that downregulation of miR-519 or upregulation of SMOC2 recovered the hsa_circ_0074298 depletion-induced and proliferation-decreased ability using PANC-1-GEM cells after treatment with 100 nM GEM for 2 days (Figure 6A). Flow cytometry analysis with FITC-conjugated Annexin V/PI staining showed that hsa_circ_0074298 depletion promoted cell apoptosis after treatment with 100 nM GEM for 48 h, but downregulated miR-519 or upregulated SMOC2 recovered the survival ability of PANC-1-GEM cells (Figure 6B and C). Overall, the results confirmed that hsa_circ_0074298 promoted PC chemoresistance by sponging miR-519 and enhancing SMOC2 expression.

Discussion

The current study suggested that hsa_circ_0074298 expression increased in both PC tissues and PC cell lines. Hsa_circ_0074298 was 1,486 bp long and constructed with part of the *HARS* gene exon. Downregulation of hsa_circ_0074298 led to cell cycle arrest at the G2/M phase, and hsa_circ_0074298 silencing suppressed cell proliferation, migration, and GEM resistance. The hsa_circ_0074298 therefore functioned in PC progression and chemoresistance. Increasing studies have found that circRNA sponges have been characterized with high expression levels and a good amount of miRNA binding sites. They are potentially effective sponges, when compared with those that are linear [17, 18]. Currently, sponging activity is the main function of some circRNAs, so in tumor development, circRNA-miRNA-mRNA interaction networks might be crucially important [19, 20].

To further identify the downstream miRNA, bioinformatics analysis was used to show that 12 different miRNAs were the targets of hsa_circ_0074298. Luciferase reporter studies confirmed that hsa_circ_0074298 could interface with miR-519. The hsa_circ_0074298 downregulation promoted miR-519 expression, and miR-519 silencing restored the proliferation, migration, and GEM resistance after hsa_circ_0074298 depletion, suggesting that miR-519 had anti-tumor activity. Previous studies also found that upregulation of miR-519 inhibited cancer cell activity, including that of nasopharyngeal carcinoma and gastric cancer [21-23]. Together, these results strongly suggested that hsa_circ_0074298 expression promoted PC progression by sponging miR-519.

Our further bioinformatics analyses showed that miR-519 bound to the SMOC2 3'-UTR, and luciferase reporter studies confirmed that miR-519 interacted with the 3'-UTR of SMOC2. Overexpression of SMOC2 restored the proliferation, migration, and GEM resistance after hsa_circ_0074298 depletion. An SMOC-2 named the SPARC-related modular calcium binding 2, which is a member of the SPARC family, is highly expressed during wound healing and embryogenesis [24-26]. Its gene product is a matricellular protein that stimulates endothelial cell migration and proliferation, and angiogenic activity [27, 28]. This study also found that targeting the cancer stem cell signature gene, *SMOC-2*, inhibited endometrial carcinoma cell proliferation and overcame the chemoresistance [29]. Smoc2 potentiates carcinoma cell proliferation through cell cycle progression promotion [15, 30]. The present investigation showed that hsa_circ_0074298 promoted PC cell proliferation, migration, and chemoresistance by sponging miR-519 and enhancing SMOC2 expression.

Conclusions

In conclusion, results verified that hsa_circ_0074298 promoted proliferation in PC cells by possibly activating miR-519/SMOC2 signaling. But the role of hsa_circ_0074298 in the metastasis of PC still needs further analysis using an *in vivo* transfer murine model in future studies. Our results indicate that hsa_circ_0074298 could be a candidate biomarker for PC prognosis and diagnosis, and may extend the use of drugs that target hsa_circ_0074298, which indicates the promising role regarding hsa_circ_0074298 in PC treatment.

Declarations

Acknowledgements

We would like to thank the researchers and study participants for their contributions.

Author Contributions

HC and DX performed all experiments and analyzed the data; HC and JZ carried out all experiments and revised the manuscript; LW and JZ designed the studies and prepared the manuscript with comments from all authors. All authors read and approved the final manuscript.

Funding

The study was funded by a grant from the National Natural Science Foundation of China (No. 81572408), and the Natural Science Foundation of Jiangsu Province, China (No. BE2015712).

Availability of data and materials

The datasets used and/or analyzed during the current study are available from the corresponding author upon reasonable request.

Ethics approval and consent to participate

The Ethics Committee of the Affiliated Zhongda Hospital of Southeast University approved this research, and the study was conducted in accordance with The Code of Ethics of the World Medical Association. All patients consented to use of resected tissues for research purposes.

Consent for publication

Not applicable.

Competing interest

The authors declare that they have no conflicts of interests.

Author details

[1]Department of Hepatic-Biliary-Pancreatic Center, Zhongda Hospital, Southeast University, Nanjing, China, 210009.

[2]Department of Hepatobiliary Surgery Research Institute, Southeast University, Nanjing, China, 210009.

Abbreviations

circRNAs, Circular RNAs; PC, pancreatic cancer; GEM, gemcitabine; ncRNAs, Non-coding RNAs; ceRNA, competing endogenous RNA; FITC, fluorescein isothiocyanate; DMEM, Dulbecco's Modified Eagle's Medium; FBS, fetal bovine serum; CCK-8, Cell Counting Kit-8; RT-qPCR, quantitative reverse transcription-polymerase chain reaction.

References

1. **Global, regional, and national life expectancy, all-cause mortality, and cause-specific mortality for 249 causes of death, 1980-2015: a systematic analysis for the Global Burden of Disease Study 2015**. *Lancet* 2016, **388**(10053):1459-1544.
2. Yoshida Y, Yamada T, Matsuoka H, Sonoda H, Fukazawa A, Yoshida H, Ishida H, Hirata K, Hasegawa S, Sakamoto K *et al*: **A Trial Protocol of Biweekly TAS-102 and Bevacizumab as Third-Line Chemotherapy for Advanced/Recurrent Colorectal Cancer: A Phase II Multicenter Clinical Trial (The TAS-CC4 Study)**. *J Anus Rectum Colon* 2019, **3**(3):136-141.
3. Schweighauser W, Pectora PM, Greenberger B, Easterner W, Wall E, Prager G, Schamber-Moser R, Grail R, Glatzer M: **Patterns of care in metastatic pancreatic cancer: patient selection in clinical routine**. *Therapy Adv Gastroenterol* 2019, **12**:1756284819877635.
4. Fujisawa N, Miyake K, Higuchi T, Oshiro H, Zhang Z, Park JH, Kawaguchi K, Chawla SP, Bouvet M, Singh SR *et al*: **Induction of Metastasis by Low-dose Gemcitabine in a Pancreatic Cancer Orthotopic Mouse Model: An Opposite Effect of Chemotherapy**. *Anticancer Res* 2019, **39**(10):5339-5344.
5. Birney E, Stamatoyannopoulos JA, Dutta A, Guigo R, Gingeras TR, Margulies EH, Weng Z, Snyder M, Dermitzakis ET, Thurman RE *et al*: **Identification and analysis of functional elements in 1% of the human genome by the ENCODE pilot project**. *Nature* 2007, **447**(7146):799-816.
6. Xie N, Liu G: **ncRNA-regulated immune response and its role in inflammatory lung diseases**. *Am J Physiol Lung Cell Mol Physiol* 2015, **309**(10):L1076-1087.
7. Ding B, Lou W, Xu L, Fan W: **Non-coding RNA in drug resistance of hepatocellular carcinoma**. *Biosci Rep* 2018, **38**(5).
8. Salmena L, Poliseno L, Tay Y, Kats L, Pandolfi PP: **A ceRNA hypothesis: the Rosetta Stone of a hidden RNA language?***Cell* 2011, **146**(3):353-358.
9. Hansen TB, Jensen TI, Clausen BH, Bramsen JB, Finsen B, Damgaard CK, Kjems J: **Natural RNA circles function as efficient microRNA sponges**. *Nature* 2013, **495**(7441):384-388.

10. Memczak S, Jens M, Elefsinioti A, Torti F, Krueger J, Rybak A, Maier L, Mackowiak SD, Gregersen LH, Munschauer M *et al*: **Circular RNAs are a large class of animal RNAs with regulatory potency**. *Nature* 2013, **495**(7441):333-338.
11. Guo JU, Agarwal V, Guo H, Bartel DP: **Expanded identification and characterization of mammalian circular RNAs**. *Genome Biol* 2014, **15**(7):409.
12. Hao L, Rong W, Bai L, Cui H, Zhang S, Li Y, Chen D, Meng X: **Upregulated circular RNA circ_0007534 indicates an unfavorable prognosis in pancreatic ductal adenocarcinoma and regulates cell proliferation, apoptosis, and invasion by sponging miR-625 and miR-892b**. *J Cell Biochem* 2019, **120**(3):3780-3789.
13. Chen G, Shi Y, Zhang Y, Sun J: **CircRNA_100782 regulates pancreatic carcinoma proliferation through the IL6-STAT3 pathway**. *Onco Targets Ther* 2017, **10**:5783-5794.
14. Xu C, Yu Y, Ding F: **Microarray analysis of circular RNA expression profiles associated with gemcitabine resistance in pancreatic cancer cells**. *Oncol Rep* 2018, **40**(1):395-404.
15. Su JR, Kuai JH, Li YQ: **Smoc2 potentiates proliferation of hepatocellular carcinoma cells via promotion of cell cycle progression**. *World J Gastroenterol* 2016, **22**(45):10053-10063.
16. Liang G, Ling Y, Mehrpour M, Saw PE, Liu Z, Tan W, Tian Z, Zhong W, Lin W, Luo Q *et al*: **Autophagy-associated circRNA circCDYL augments autophagy and promotes breast cancer progression**. *Mol Cancer* 2020, **19**(1):65.
17. Wilusz JE, Sharp PA: **Molecular biology. A circuitous route to noncoding RNA**. *Science* 2013, **340**(6131):440-441.
18. Li J, Yang J, Zhou P, Le Y, Zhou C, Wang S, Xu D, Lin HK, Gong Z: **Circular RNAs in cancer: novel insights into origins, properties, functions and implications**. *Am J Cancer Res* 2015, **5**(2):472-480.
19. Liu J, Song S, Lin S, Zhang M, Du Y, Zhang D, Xu W, Wang H: **Circ-SERPINE2 promotes the development of gastric carcinoma by sponging miR-375 and modulating YWHAZ**. *Cell Prolif* 2019, **52**(4):e12648.
20. Liu G, Shi H, Deng L, Zheng H, Kong W, Wen X, Bi H: **Circular RNA circ-FOXM1 facilitates cell progression as ceRNA to target PPDPF and MACC1 by sponging miR-1304-5p in non-small cell lung cancer**. *Biochem Biophys Res Commun* 2019, **513**(1):207-212.
21. Yu G, Zhang T, Jing Y, Bao Q, Tang Q, Zhang Y: **miR-519 suppresses nasopharyngeal carcinoma cell proliferation by targeting oncogene URG4/URGCP**. *Life Sci* 2017, **175**:47-51.
22. Abdelmohsen K, Kim MM, Srikantan S, Mercken EM, Brennan SE, Wilson GM, Cabo R, Gorospe M: **miR-519 suppresses tumor growth by reducing HuR levels**. *Cell Cycle* 2010, **9**(7):1354-1359.
23. Zhou N, Zhou Y, Tang Y, Yu W: **[MiR-519 inhibits gastric cancer cell activity through regulation of HuR expression]**. *Zhong Nan Da Xue Xue Bao Yi Xue Ban* 2016, **41**(1):19-23.
24. Pazin DE, Albrecht KH: **Developmental expression of Smoc1 and Smoc2 suggests potential roles in fetal gonad and reproductive tract differentiation**. *Dev Dyn* 2009, **238**(11):2877-2890.

25. Rocnik EF, Liu P, Sato K, Walsh K, Vaziri C: **The novel SPARC family member SMOC-2 potentiates angiogenic growth factor activity**. *J Biol Chem* 2006, **281**(32):22855-22864.
26. Vannahme C, Gosling S, Paulsson M, Maurer P, Hartmann U: **Characterization of SMOC-2, a modular extracellular calcium-binding protein**. *Biochem J* 2003, **373**(Pt 3):805-814.
27. Nishimoto S, Hamajima Y, Toda Y, Toyoda H, Kitamura K, Komurasaki T: **Identification of a novel smooth muscle associated protein, smap2, upregulated during neointima formation in a rat carotid endarterectomy model**. *Biochim Biophys Acta* 2002, **1576**(1-2):225-230.
28. Maier S, Paulsson M, Hartmann U: **The widely expressed extracellular matrix protein SMOC-2 promotes keratinocyte attachment and migration**. *Exp Cell Res* 2008, **314**(13):2477-2487.
29. Lu H, Ju DD, Yang GD, Zhu LY, Yang XM, Li J, Song WW, Wang JH, Zhang CC, Zhang ZG *et al*: **Targeting cancer stem cell signature gene SMOC-2 Overcomes chemoresistance and inhibits cell proliferation of endometrial carcinoma**. *EBioMedicine* 2019, **40**:276-289.
30. Shvab A, Haase G, Ben-Shmuel A, Gavert N, Brabletz T, Dedhar S, Ben-Ze'ev A: **Induction of the intestinal stem cell signature gene SMOC-2 is required for L1-mediated colon cancer progression**. *Oncogene* 2016, **35**(5):549-557.

Figures

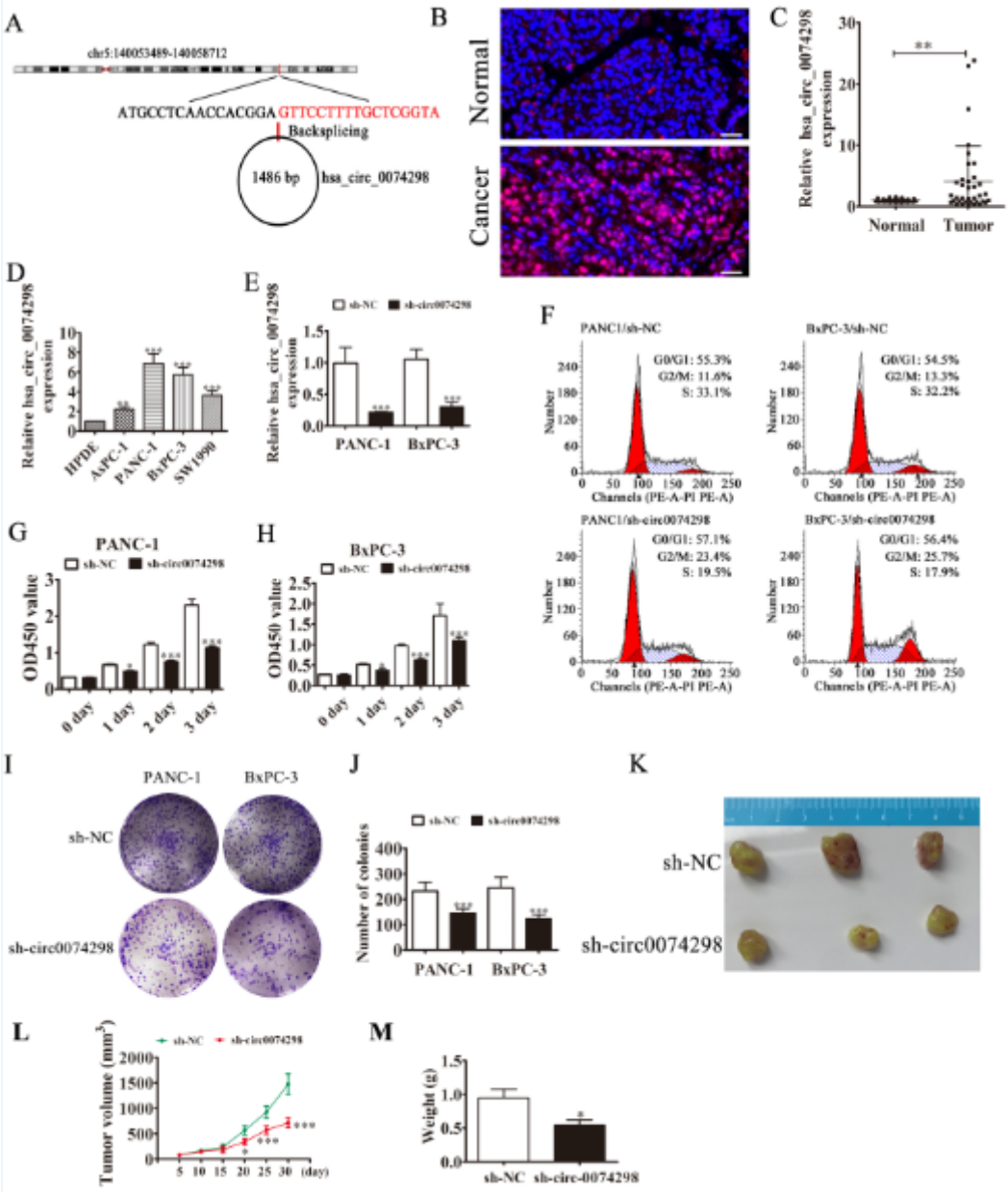

Figure 1

Knockdown of hsa_circ_0074298 suppressed pancreatic cancer (PC) proliferation both in vivo and in vitro. (A) The genomic loci of the HARS gene and hsa_circ_0074298. (B) The expression and subcellular localization of hsa_circ_0074298 in PC tissue was analyzed using in situ hybridization. Scale bar: 50 μm. (C) RT-qPCR showed the expression of hsa_circ_0074298 in PC tissue. Data are presented as the mean ± SD. **P < 0.01 vs. normal. (D) RT-qPCR showed the expression of hsa_circ_0074298 in PC cell lines (PANC-1, SW1990, BxPC-3, and AsPC-1) and in normal human pancreatic duct epithelial (HPDE) cells. Data are presented as the mean ± SD. **P < 0.01; ***P < 0.001 vs. normal cells. (E) RT-qPCR detection of hsa_circ_0074298 expression in both PANC-1 and BxPC-3 cells following transfection with siRNA against hsa_circ_0074298 (sh-circ0074298) or the negative control (NC). Data are presented as the mean ± SD. ***P < 0.001 vs. NC. (F) Flow cytometry detection showing the percentages of cells in G1, S, or G2 phase in both PANC-1 and BxPC-3 cells. (G and H) The CCK8 assay shows the cell proliferation of both PANC-1

(G) and BxPC-3 (H) cells. Data are presented as the mean ± SD. *P < 0.05; ***P < 0.001 vs. NC. (I and J) The colony formation assay showing proliferation in both PANC-1 and BxPC-3 cells. Data are presented as the mean ± SD; ***P < 0.001 vs. NC. (K) Knockdown of hsa_circ_0074298 attenuated PANC-1 tumor growth in xenografts of nude mice. (L and M) Tumor volume (L) and weight (M) were calculated. Data are presented as the mean ± SD. *P < 0.05; ***P < 0.001 vs. NC.

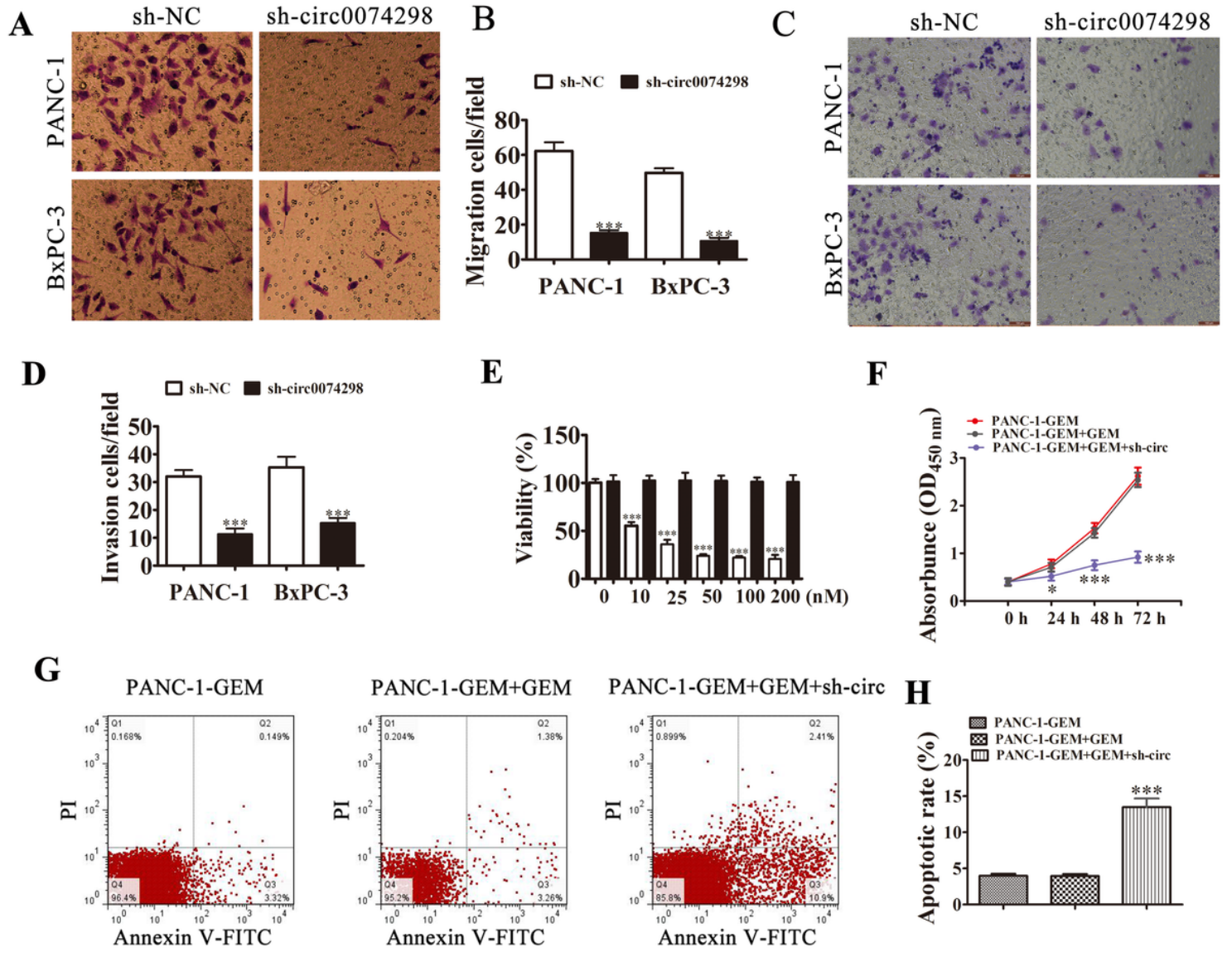

Figure 2

Knockdown of hsa_circ_0074298 decreased the migration capabilities and gemcitabine (GEM) resistance in pancreatic cancer (PC). (A-D) The Transwell assay showed the migration (A and B) and invasion (C and D) of both PANC-1 and BxPC-3 cells. Data are presented as the mean ± SD; ***P < 0.001 vs. the normal control (NC). (E) PANC-1 cells and the derived long-time GEM-treated subclone PANC-1-GEM were untreated (0 nM) or treated with GEM with concentrations from 10 to 200 nM as indicated. The viability was measured by the CCK8 assay, 48 h after treatment. Data are presented as the mean ± SD; ***P < 0.001 vs. the untreated group. (F) The CCK8 assays were used to evaluate the cellular proliferation of PANC-1-GEM cells with or without hsa_circ_0074298 silencing after treatment with 100 nM GEM for

different times (0–72 h). Data are presented as the mean ± SD; ***P < 0.001 vs. the untreated group. (G and H) PANC-1-GEM cells with or without hsa_circ_0074298 silencing were treated with 100 nM GEM followed by staining with Annexin V-FITC and propidium iodide 48 h later, then evaluated by FACS-analysis. The percentage of FITC-positive cells is shown as “Apoptosis rate (%).” Data are presented as the mean ± SD; ***P < 0.001 vs. the untreated group.

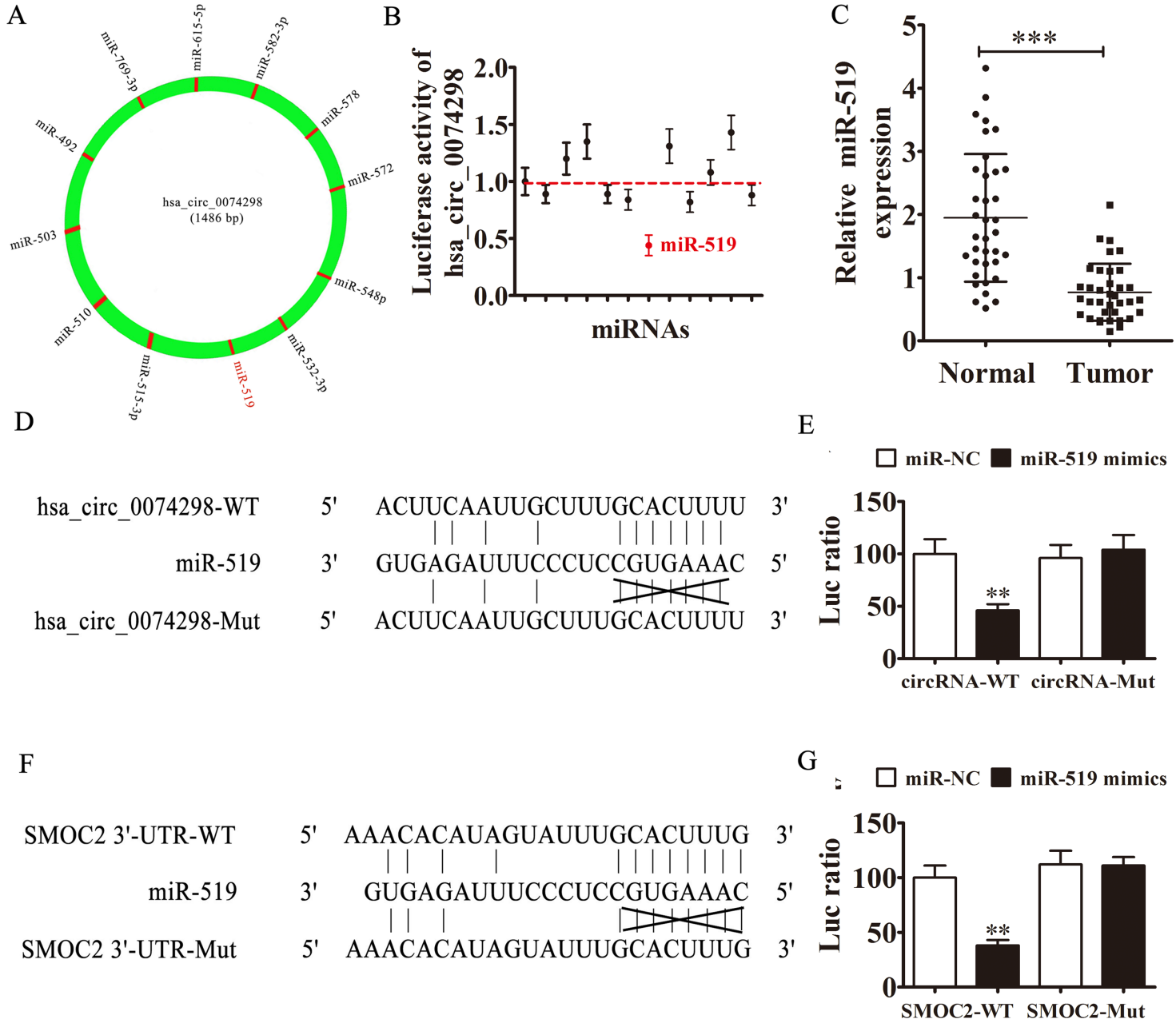

Figure 3

The miR-519/SMOC2 was the target of hsa_circ_0074298. (A) A schematic model showing the putative binding sites of 12 predicted miRNAs on hsa_circ_0074298. (B) The luciferase activity of hsa_circ_0074298 in HEK293T cells transfected with miRNA mimics, which are putative binding sites for the hsa_circ_0074298 sequence. Luciferase activity was normalized by Renilla luciferase activity. (C) RT-qPCR showing the relative expression of the miR-519 from pancreatic cancer tumor tissues and adjacent

non-tumor tissues. Data are presented as the mean ± SD. ***P < 0.001. (D) The predicted binding sites of miR-519 in the hsa_circ_0074298. The mutated (Mut) version of hsa_circ_0074298 is also shown. (E) Relative luciferase activity was determined 48 h after transfection with miR-519 mimic/normal control (NC) or with the hsa_circ_0074298 wild-type/Mut in HEK293T cells. Data are presented as the mean ± SD; **P < 0.01. (F) The predicted binding sites of miR-519 within the 3'-UTR of SMOC2. The mutated version of the 3'-UTR of SMOC2 is also shown. (G) Relative luciferase activity was determined 48 h after transfection with the miR-519 mimic/normal control or with the 3'-UTR-SMOC2 wild-type/Mut in HEK293T cells. Data are presented as the mean ± SD; **P < 0.01.

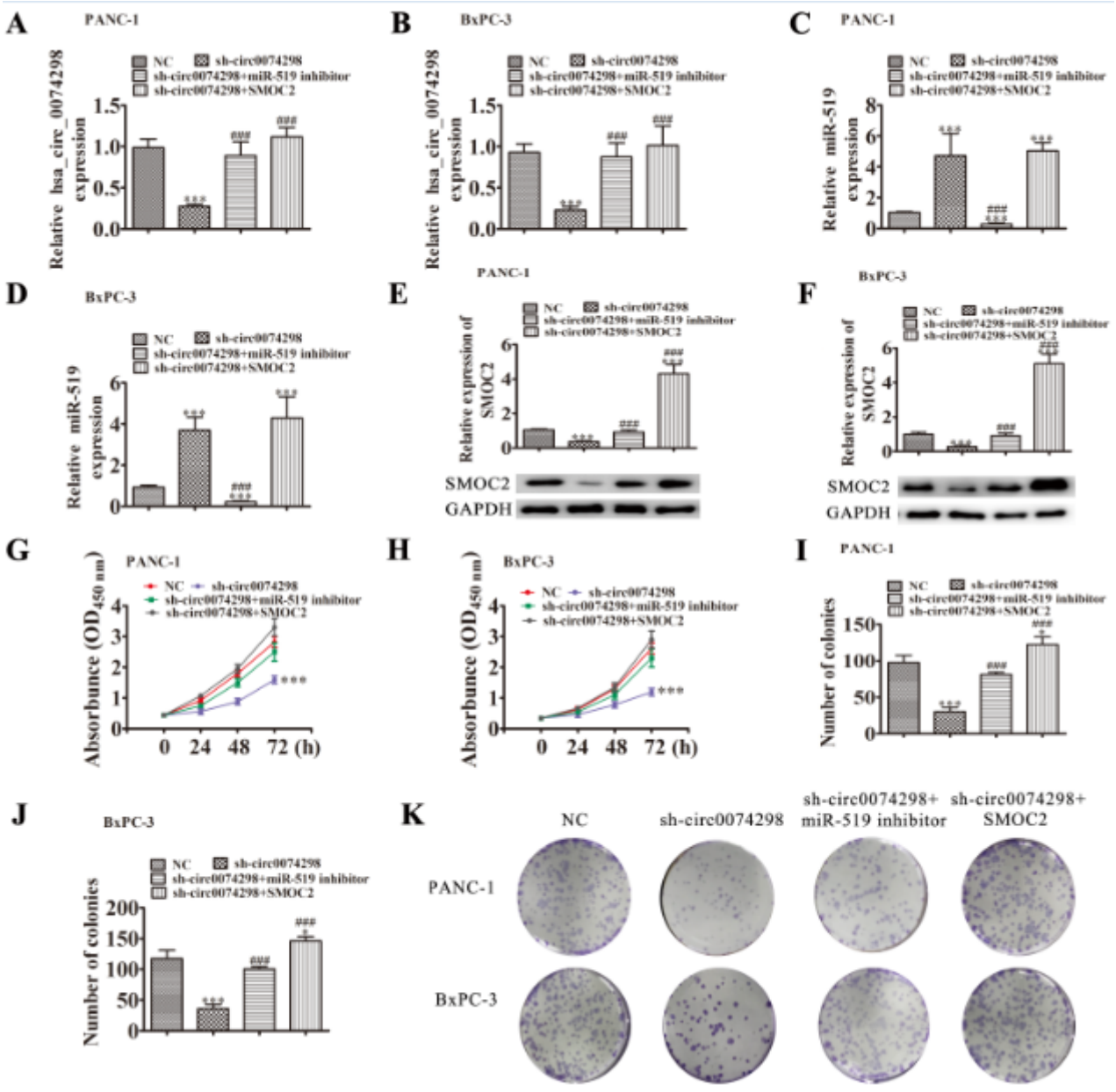

Figure 4

Overexpression of miR-519 or downregulation of SMOC2 reversed the proliferation ability after hsa_circ_0074298 silencing in pancreatic cancer (PC) cells. (A-D) RT-qPCR detection showing the expression of hsa_circ_0074298 (A and B) and miR-519 (C and D) in PANC-1 and BxPC-3 cells. Data are

presented as the mean ± SD; ***P < 0.001 vs. NC; ###P < 0.001 vs. sh-circ0074298. (E and F) Western blot analysis showing the expressions of SMOC2 in PANC-1 and BxPC-3 cells. Data are presented as the mean ± SD; ***P < 0.001 vs. NC; ###P < 0.001 vs. sh-circ0074298. (G and H) CCK8 assays were used to evaluate cell proliferation after 72 h of culture. Data are presented as the mean ± SD; ***P < 0.001 vs. NC; ###P < 0.001 vs. sh-circ0074298. (I-K) Colony formation assays showing the proliferation of PANC-1 and BxPC-3 cells. Data are presented as the mean ± SD; *P < 0.05; ***P < 0.001 vs. NC; ###P < 0.001 vs. sh-circ0074298.

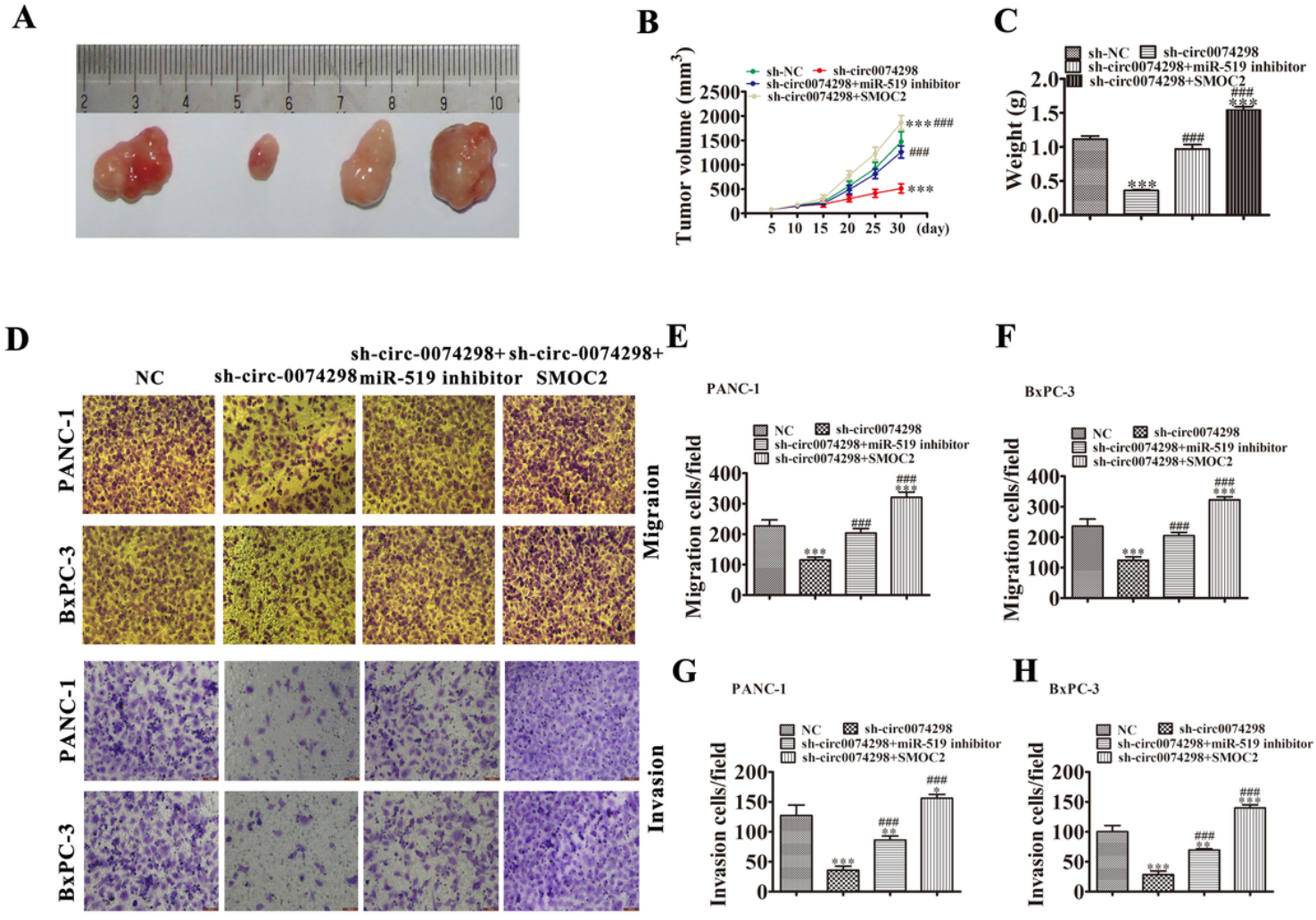

Figure 5

Overexpression of miR-519 or downregulation of SMOC2 reversed the growth and migration ability after hsa_circ_0074298 silencing of pancreatic cancer (PC) cells. (A) Xenograft tumors in nude mice from the four treatment groups (NC, sh-circRNA, sh-circRNA + miR-519 inhibitor, and sh-circRNA + SMOC2) after subcutaneous injection of PANC-1 cells. (B and C) Xenograft volumes (B) and weight (C) from the four treatment groups were measured at the indicated time points. Data are presented as the mean ± SD. ***P < 0.001 vs. the NC; ###P < 0.001 vs. sh-circ0074298. (D-H) Cell migration and invasion were assessed in PANC-1 and BxPC-3 cells using Transwell assays. Data are presented as the mean ± SD; ***P < 0.001 vs. NC; ###P < 0.001 vs. sh-circ0074298.

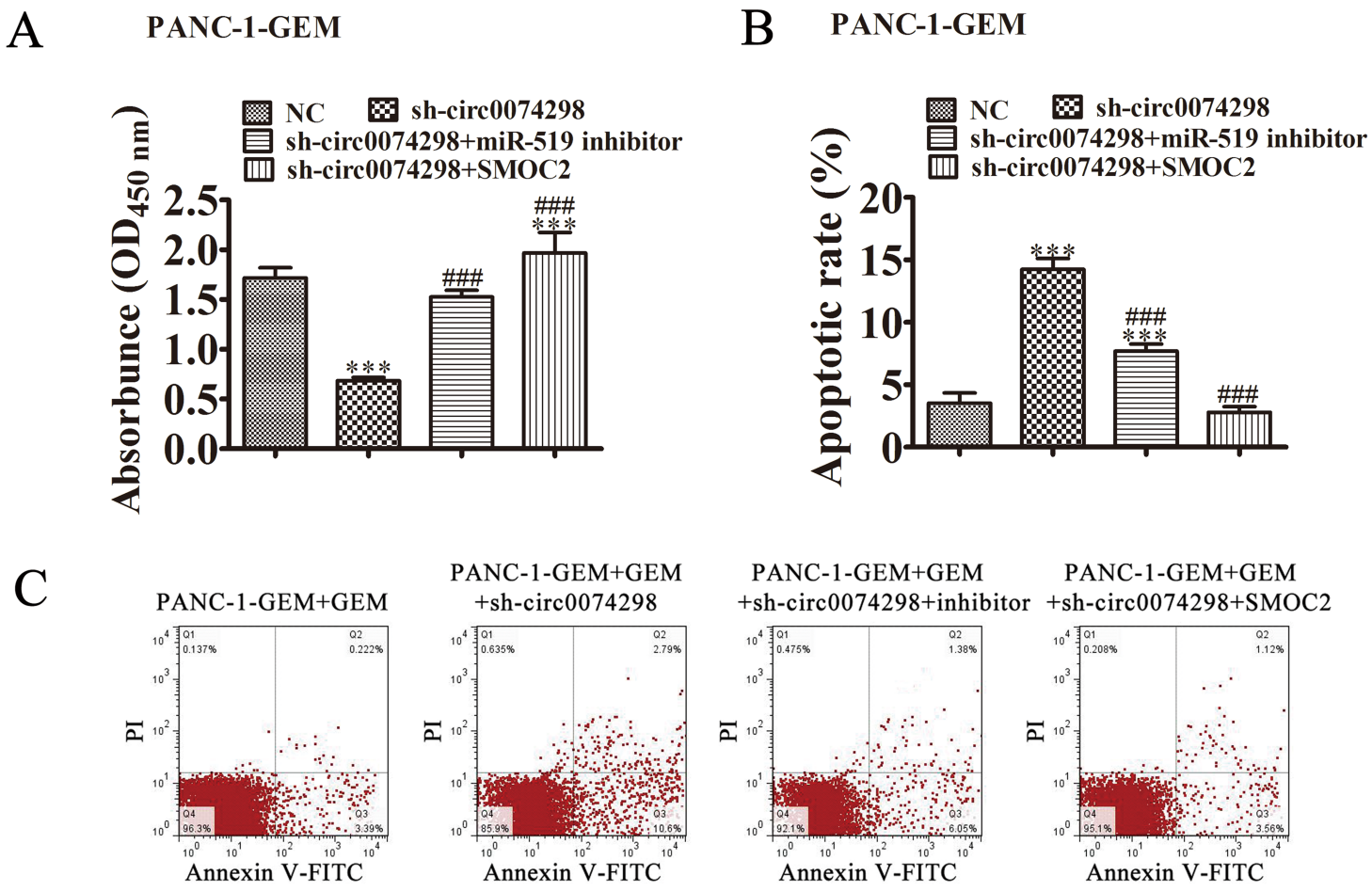

Figure 6

The miR-519/SMOC2 was the target of hsa_circ_0074298. (A) A schematic model showing the putative binding sites of 12 predicted miRNAs on hsa_circ_0074298. (B) The luciferase activity of hsa_circ_0074298 in HEK293T cells transfected with miRNA mimics, which are putative binding sites for the hsa_circ_0074298 sequence. Luciferase activity was normalized by Renilla luciferase activity. (C) RT-qPCR showing the relative expression of the miR-519 from pancreatic cancer tumor tissues and adjacent non-tumor tissues. Data are presented as the mean ± SD. ***P < 0.001. (D) The predicted binding sites of miR-519 in the hsa_circ_0074298. The mutated (Mut) version of hsa_circ_0074298 is also shown. (E) Relative luciferase activity was determined 48 h after transfection with miR-519 mimic/normal control (NC) or with the hsa_circ_0074298 wild-type/Mut in HEK293T cells. Data are presented as the mean ± SD; **P < 0.01. (F) The predicted binding sites of miR-519 within the 3'-UTR of SMOC2. The mutated version of the 3'-UTR of SMOC2 is also shown. (G) Relative luciferase activity was determined 48 h after transfection with the miR-519 mimic/normal control or with the 3'-UTR-SMOC2 wild-type/Mut in HEK293T cells. Data are presented as the mean ± SD; **P < 0.01.